A Tight-Binding Model for Illustrating Exciton Confinement in Semiconductor Nanocrystals

Z. Hens, Christophe Delerue

A Tight-Binding Model for Illustrating Exciton Confinement in Semiconductor Nanocrystals

Z. Hens[1, a)] and C. D. Delerue[2]
[1)] *Physics and Chemistry of Nanostructures, Ghent University, 9000 Gent, Belgium*
[2)] *Université de Lille, CNRS, Université Polytechnique Hauts-de-France, Junia, UMR 8520 - IEMN, F-59000 Lille, France*

(*Electronic mail: zeger.hens@ugent.be)

(Dated: 21 February 2024)

The Brus equation describes the relation between the lowest energy of an electron-hole pair and the size of a semiconductor crystallite. However, taking the strong confinement regime as a starting point, the equation does not cover the transition from weak to strong confinement, the accompanying phenomenon of charge-carrier delocalization, or the change in the transition dipole moment of the electron-hole pair state. Here, we use a one-dimensional (1D), two-particle Hubbard model for interacting electron-hole pairs that extends the well-known tight-binding Hueckel approach through a point-like electron-hole interaction. On infinite chains, the resulting exciton states exhibit the known relation between the Bohr radius, the exciton binding energy and the effective mass of the charge carriers. Moreover, by introducing infinite-well boundary conditions, the model enables the transition of the exciton states from weak to strong confinement to be tracked, while straightforward adaptations provide insight in the relation between defects, exciton localization, and confinement. In addition, by introducing the dipole operator, the variation of the transition dipole moment can be mapped when shifting from electron-hole pairs in strong confinement to delocalized and localized excitons in weak confinement. The proposed model system can be readily implemented and extended to different multi-carrier states, thus providing researchers a tool for exploring, understanding and teaching confinement effects in semiconductor nanocrystals under different conditions.

I. INTRODUCTION

In two seminal papers published about 40 years ago, Louis Brus described the impact of size on the energy levels of spherical semiconductor crystallites.[1,2] These studies led to the formulation of what became the Brus equation; an expression that describes the impact of quantum confinement and Coulomb interaction on the lowest energy ε_{gap} of the electron-hole pair in a semiconductor crystallite. This equation is mostly reproduced as:[3]

$$\varepsilon_{gap} = \varepsilon_{gap,\infty} + \frac{\hbar\pi^2}{2R^2}\left(\frac{1}{m_e^\star} + \frac{1}{m_h^\star}\right) - 1.8\frac{e^2}{4\pi\varepsilon_0\varepsilon R} \qquad (1)$$

Here, all symbols have there usual meaning, while R denotes the radius of the nanocrystal, and $\varepsilon_{gap,\infty}$, $m_e^\star$, $m_h^\star$ and ε are the band gap, the effective masses of the electron and the hole, and the dielectric constant of the semiconductor at hand, respectively. In Eq 1, the first R-dependent term describes the increase in kinetic energy caused by the confinement of the electron-hole pair, while the second is the electron-hole Coulomb interaction. What Brus highlighted in his work, is that for radii of a few nanometer, the R^{-2} scaling will make the confinement energy the dominant contribution to the energy of the electron-hole pair, a characteristic that defines the regime of strong confinement.[3]

Brus derived Eq 1 using first order perturbation theory, starting from the assumption that the confinement energy was dominant. In that respect, Eq 1 is self-consistent – confirming the initial assumption – but does not describe the gradual change of the energy of the electron-hole pair when reducing the crystal size. This change includes, for example, the weak confinement regime, in which the Coulomb interaction is largest and confinement mostly affects the bound electron-hole pair, i.e., the exciton, rather than the separate charge carriers.[3] This point was recognized by Brus,[2] yet opposite from the strong confinement regime, the analysis of weak confinement he put forward did not transpire into a single equation that is readily reproduced in papers, textbooks or dissertations.

Interestingly, Louis Brus developed his theory on strong confinement in the context of the redox potentials of small semiconductor crystallites,[1] a chemical problem that remains relevant today in view of photocatalysis and electrocatalysis by nanocrystals.[4] This interplay between physics and chemistry remained a key characteristic of the field of colloidal quantum dots, which quickly developed in the years following the pioneering work of Louis Brus.[5] More recently, interest has been extending from semiconductor nanocrystals in strong confinement to larger nanocrystals exhibiting excitons in weak confinement or, at room temperature, bulk characteristics. Examples include three-dimensional nanocrystals of lead halide perovskites or cadmium chalcogenides,[6–8] and two-dimensional nanocrystals that can be synthesized as colloidal nanoplatelets with atomically-precise thicknesses,[9]. Bulk CdS nanocrystals, for example, where recently shown to have exceptional promise as an optical gain material,[8] while $CsPbBr_3$ nanocrystals have been put forward as sources of indistinguishable single photons.[7] Nanoplatelets, on the other hand, feature strong quantization out of plane and weak or no in-plane quantization, which leads to the formation of

[a)] Also at Center for Nano and Biophotonics, Ghent University, 9000 Gent, Belgium

two-dimensional excitons. The giant oscillator strength of such excitons leaves a clear imprint in the absorption spectrum, but does not translate into ultrafast exciton recombination at room temperature; an inconsistency indicative of exciton localization.[10] Similar difference betwee absorption and emission were observed on larger epitaxial nanocrystals,[11] but are absent for nanocrystals in strong confinement.[12] So weakly confined excitons have markedly different properties than strongly confined electron-hole pairs. While these diverging characteristics of excitons in weak confinement are not unexpected, they fall outside the scope of the simplified approaches used to teach size quantization, such as Eq 1. In this way, the emerging interest in excitons in bulk nanocrystals creates a need for a simple model system that can illustrate the concept of size quantization in full – from weak to strong confinement – to the broad field of researchers working on confined semiconductor nanocrystals.

In this work, we use a one-dimensional (1D) description of electron-hole pair states to discuss the interplay between size, electron-hole interaction and deviations from periodicity on the states of the electron-hole pair. The approach involves a two-particle Hubbard model that extends the well-known Hückel or tight-binding analysis of single electron states on a 1D chain to states of an interacting electron-hole pair. Implementing a point-like electron-hole interaction, we obtain an analytical solution for the delocalized, bound exciton state that illustrates the relation between the exciton Bohr radius, the exciton binding energy and the effective mass of the charge carriers. Next, we map the transition from weak to strong confinement by reducing the length of the chain, which eventually makes the bound exciton resemble a free electron-hole pair. Next, we introduce a deviation from the crystal periodicity to discuss localization of excitons, and the impact of localization on the confinement regime. Finally, we use the different model systems – free electron-hole pair, delocalized and localized exciton – to track the variation of the transition dipole moment of the exciton as a function of the chain length and the electron-hole interaction. Given the surprisingly rich variety of exciton properties that can be addressed, the tight-binding Hueckel model presented here can help researchers in the field of confined semiconductors to better understand and explore the properties of confined excitons, for which the Brus equation provided a first description in the regime of strong confinement.

II. DESCRIPTION OF ELECTRON-HOLE PAIR STATES

A. General Concepts

The model introduced here is a one-dimensional (1D), two-particle Hubbard model that extends the tight-binding Hückel approach for calculating single-electron states on a 1D chain of atoms to electron-hole pair states. A similar approach was used to highlight the distinction between Wannier and Frenkel excitons on infinite chains,[13] or to describe oscillator strengths and higher harmonic generation in semiconductor nanostructures.[14,15] For simplicity, we use the following assumptions:

1. The lattice parameter is set at $d = 1$, effectively taking d as the unit of length.

2. States $|\,a_s\,\rangle$ and $|\,b_t\,\rangle$ are considered that represent an electron on atom s and a hole on atom t, respectively. The underlying atomic orbitals have even parity, and the on-site matrix elements are denoted as:

$$\langle\, a_s \,|\, \mathbf{H}_e \,|\, a_s \,\rangle = \varepsilon_a \tag{2}$$
$$\langle\, b_t \,|\, \mathbf{H}_h \,|\, b_t \,\rangle = \varepsilon_b \tag{3}$$

   Here, $\mathbf{H}_e$ and $\mathbf{H}_h$ are the Hamiltonian operators for the electron and hole energy, respectively.

3. Only nearest-neighbor coupling is taken as non-zero, with the hopping matrix element defined for any s and t as:

$$\langle\, a_{s-1} \,|\, \mathbf{H}_e \,|\, a_s \,\rangle = V \tag{4}$$
$$\langle\, b_{t-1} \,|\, \mathbf{H}_h \,|\, b_t \,\rangle = V \tag{5}$$

The approach to obtain single-particle eigenstates for such a chain, and link the results to properties of real, 3D semiconductors, is discussed in many textbooks,[16] and is detailed in Appendix A for completeness. Note that the hopping matrix element V is inversely proportional to the effective mass. Hence, taking V identical for electrons and holes describes a system where both charge carriers have the same effective mass. This assumption simplifies the analysis, but the extension of the approach to electrons and holes with different effective masses is straightforward. In this section, we outline the characteristics of the electron-hole pair eigenstates for infinite chains, with the aim of introducing a common terminology for describing the eigenstates and a view on the exciton properties. These results will help rationalize the impact of size quantization and localization on the opto-electronic properties of the exciton states in the following sections. More extensive discussions of the Hubbard model can be found in specialized texts.[17]

B. Atom-Localized Electron-Hole Pair States

Extending the notion of single-electron states, we introduce a set of basis states $|\,a_s, b_t\,\rangle$ for electron-hole pairs as the direct product of the electron state $|\,a_s\,\rangle$ and the hole state $|\,b_t\,\rangle$. As outlined in Figure 1a, these states represent an electron localized on atom s and a hole on atom t, respectively. Figure 1b illustrates that the electron and hole position can be equally set using the center-of-mass R of the electron-hole pair and the electron-hole distance r, two quantities defined in terms of s and t as:

$$\begin{array}{c} R = \frac{1}{2}(s+t) \\ r = s-t \end{array} \quad \Leftrightarrow \quad \begin{array}{c} s = R + \frac{r}{2} \\ t = R - \frac{r}{2} \end{array} \tag{6}$$

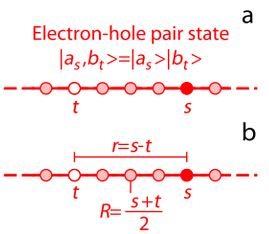

FIG. 1. Spatial coordinates for describing atom-localized electron-hole pairs. (a) Definition of electron-hole pair state $|a_s,b_t\rangle$ on the 1D atom chain as the direct product of the single-electron state $|a_s\rangle$ and the single-hole state $|b_t\rangle$, which represent an electron localized an atom s and a hole on atom t, respectively. (b) Relation between the electron and hole coordinates s and t, and the electron-hole center of mass coordinate R and the electron-hole interdistance r.

Therefore, the state $|R,r\rangle$ featuring an electron-hole pair with center-of-mass R and electron-hole distance r is identical to the atom-localized electron-hole pair state defined as:

$$|R,r\rangle = |a_{R+\frac{r}{2}},b_{R-\frac{r}{2}}\rangle \tag{7}$$

As outlined in Appendix B, conjugate wavenumbers K and κ can be defined for the coordinates R and r.

The N^2 atom-localized states $|a_s,b_t\rangle$ can be used as a basis to construct the electron-hole pair Hamiltonian matrix, and find the actual electron-hole pair eigenstates as linear combinations of the atom-localized states. This approach has several advantages. The electron-hole pair Hamiltonian matrix is readily expressed in terms of the single-particle on-site and hopping matrix elements, and the implementation of infinite-wall boundary conditions for a finite chain is straightforward. On the other hand, this brute-force approach involves a Hamiltonian with dimensions scaling like N^2, and does not give extensive insight in the properties of the eigenstates. To overcome both drawbacks, we will first design states in agreement with the translational symmetry of the atom chain and then construct for each symmetry-adapted subset of states a Hamiltonian matrix with lower dimensions.

C. Symmetry-Adapted Electron-Hole Pair States

To understand the characteristics of symmetry adapted electron/hole pair states, consider the atom-localized state $|a_s,b_s\rangle$, which consists of an electron and a hole co-localized on the same atom s. Such a state could be an eigenstate if electron-hole attraction is the dominant interaction. However, a leftward shift of the chain by a lattice parameter changes $|a_s,b_s\rangle$ into $|a_{s-1},b_{s-1}\rangle$, a different state. Given this lack of invariance under translation, $|a_s,b_s\rangle$ cannot be an electron-hole pair eigenstate on the infinite chain. On the other hand, using the same approach to create translation-invariant single-particle states, see Appendix A, a co-localized electron-hole pair state $|K,\nu\rangle$ that transforms correctly under translation can be constructed as:

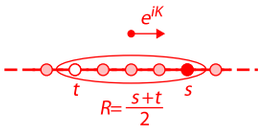

FIG. 2. Representation of the procedure to form electron-hole pair states in line with the translation symmetry of the atom chain, involving the addition of shifted copies of a fixed combination of atom-localized states – only one is shown – where a shift by a lattice parameter involves a multiplication by a phase factor e^{iK}.

$$|K,\nu\rangle = \frac{1}{\sqrt{N}}\sum_s e^{i(k+l)\cdot s}|a_s,b_s\rangle = \sum_s e^{iK\cdot R}|a_R,b_R\rangle \tag{8}$$

Here, we introduced k and l as the electron and hole wavenumbers, see Appendix A, we identified s with the center-of-mass R of the electron-hole pair, and used ν as a label for the internal state – the co-localized electron and hole – of the electron-hole pair. Note that the phase shift of the state $|K,\nu\rangle$ upon translation by a single lattice parameter is determined by $k+l$, a sum of wavenumbers. As shown in Appendix B, this sum can be interpreted as the wavenumber K conjugate to the center-of-mass R of the electron-hole pair. Note that K acts as a quantum number that characterizes an electron-hole pair state adapted to the symmetry of the crystal.

To appreciate the difference between an electron-hole pair state such as $|K,\nu\rangle$ and an atom-localized state $|a_s,b_s\rangle$, three elements are important:

1. While $|a_s,b_s\rangle$ is localized on a single atom, the state $|K,\nu\rangle$ is fully delocalized across the entire chain. This characteristic is essential in view of the required invariance of the eigenstates under translations of the chain.

2. Opposite from the atom-localized electron-hole pair state $|a_s,b_s\rangle$, the state $|K,\nu\rangle$ cannot be written as a direct product of an electron and a hole state, but is an inseparable linear combination of such states.

3. While fully delocalized across the entire chain of atoms, the position of the electron and the hole in the state $|K,\nu\rangle$ are strongly correlated. In fact, by the extreme choice of constructing the exciton using states localized on the same atom, knowing the position of one carrier removes all uncertainty on the position of the other carrier.

While $|K,\nu\rangle$ transforms correctly under a translation of the chain, the state will only be an electron-hole pair eigenstate in the specific case where the electron-hole attraction is the dominant energy term, *vide infra*. Even so, given the requirement of translational symmetry, the actual eigenstates will have a similar structure. As outline in Figure 2, a first part consists of the linear combination of atom-localized electron-hole pair states with a given center-of-mass R. This will yield N linearly independent combinations that can be characterized by the internal quantum number ν. A second part involves the addition

of shifted copies of this state, each weighed by the phase factor $\exp(iKR)$, where K serves as a second quantum number. As there will be N center-of-mass wavenumbers, there is indeed room for N^2 eigenstates.

Implementing these principles, the following expansion for any electron-hole pair eigenstate $|K,\nu\rangle$ on an infinite chain can be put forward:

$$|K,\nu\rangle = \sum_R e^{iKR}\left(\sum_r \psi_\nu(r)|a_{R+\frac{r}{2}},b_{R-\frac{r}{2}}\rangle\right) \tag{9}$$

For a given eigenstate, $\psi_\nu(r)$ is the expansion coefficient for an atom-localized basis state where the electron and the hole are separated by a distance r. Hence, the set of coefficients $\psi_\nu(r)$ can be interpreted as the internal wavefunction of the electron-hole pair state, and only an $N\times N$ internal Hamiltonian matrix is needed to determine the N internal eigenstates of the electron-hole pair.

D. The Internal Hamiltonian of the Electron-Hole Pair

Given the symmetry-adapted formulation of the eigenstates, see Eq 9, we will express the Hamiltonian using basis states $|K,r\rangle$ characterized by a center-of-mass wavenumber K and an electron hole pair separated by an interdistance r:

$$|K,r\rangle = \frac{1}{\sqrt{N}}\sum_R e^{iKR}|a_{R+\frac{r}{2}},b_{R-\frac{r}{2}}\rangle \tag{10}$$

For a given center-of-mass wavenumber K, the different elements $\mathbf{H}_{pq}$ of the Hamiltonian matrix can be written as:

$$\begin{aligned}\mathbf{H}_{K;p,q} &= \langle K,p|\mathbf{H}|K,q\rangle = \frac{1}{N}\sum_{R_1,R_2} e^{iK(R_1-R_2)} \\ &\times\langle a_{R_2+\frac{p}{2}},b_{R_2-\frac{p}{2}}|\mathbf{H}|a_{R_1+\frac{q}{2}},b_{R_1-\frac{q}{2}}\rangle\end{aligned} \tag{11}$$

In line with the construction of the single-particle Hamiltonian – see Appendix A – we assume that the matrix elements $\langle a_{R_2+\frac{p}{2}},b_{R_2-\frac{p}{2}}|\mathbf{H}|a_{R_1+\frac{q}{2}},b_{R_1-\frac{q}{2}}\rangle$ between the atom-localized states will be different from zero only in the following cases:

- *On-site matrix element.* This involves matrix elements $\langle a_s,b_t|\mathbf{H}|a_s,b_t\rangle$ that involve the same atom-localized states $|a_s,b_t\rangle$ as ket and bra, featuring an electron on atom s and a hole on atom t. Due to electron-hole interaction, the on-site matrix element can depend on the electron-hole interdistance $r=s-t$.

- *Hopping matrix element.* This involves matrix elements such as $\langle a_{s+1},b_t|\mathbf{H}|a_s,b_t\rangle = V$, where either the electron or the hole are on nearest neighbor atoms, while the other carrier is on the same atom. For simplicity, we will use a single hopping energy V in this work that is independent of the electron-hole interdistance.

Using these assumptions, one readily shows that the only non-vanishing matrix elements of the electron-hole Hamiltonian at given K are:

$$\mathbf{H}_{K;p,p} = \varepsilon_{eh}(p) \tag{12}$$

$$\mathbf{H}_{K;p+1,p} = 2V\cos\left(\frac{K}{2}\right) \tag{13}$$

$$\mathbf{H}_{K;p-1,p} = 2V\cos\left(\frac{K}{2}\right) \tag{14}$$

Hence, by labeling the rows and columns by the internal coordinate r for the N atom chain, we obtain the following internal electron-hole pair Hamiltonian matrix:

$$\mathbf{H}_K = \begin{pmatrix} & \vdots & \vdots & \vdots & \\ \cdots & \varepsilon_{eh}(-1) & 2V\cos\left(\frac{K}{2}\right) & 0 & \cdots \\ \cdots & 2V\cos\left(\frac{K}{2}\right) & \varepsilon_{eh}(0) & 2V\cos\left(\frac{K}{2}\right) & \cdots \\ \cdots & 0 & 2V\cos\left(\frac{K}{2}\right) & \varepsilon_{eh}(1) & \cdots \\ & \vdots & \vdots & \vdots & \end{pmatrix} \tag{15}$$

Appendix C generalizes this internal Hamiltonian to the description of electron-hole pairs with different hopping matrix elements for the electron and the hole, a situation corresponding to different effective masses for both charge carriers.

III. EXAMPLES OF ELECTRON-HOLE PAIR STATES

A. Free Electron-Hole Pairs

Absent any electron-hole interaction, the on-site electron-hole energy ε_{eh} will be independent of the electron-hole interdistance, and equal to $\varepsilon_a+\varepsilon_b$. The resulting Hamiltonian $\mathbf{H}_{K,kin}$ measures the kinetic energy of the relative motion of the electron-hole pair, and is formally identical to the Hamiltonian of a single electron on a chain discussed in Appendix A. Hence, the expansion coefficients $\psi_\nu(r)$ will be the phase factors of running waves, for which the internal wavenumber κ, see Appendix B, serves as the quantum number. Given the K-dependent coupling in $\mathbf{H}_K$, the energy $\varepsilon_{K,\kappa}$ of these eigenstates is then obtained as:

$$\begin{aligned}\varepsilon_{K,\kappa} &= \varepsilon_a+\varepsilon_b+4V\cos\left(\frac{K}{2}\right)\cos(\kappa) \\ &= \varepsilon_a+\varepsilon_b+2V\cos\left(\frac{K}{2}+\kappa\right)+2V\cos\left(\frac{K}{2}-\kappa\right)\end{aligned} \tag{16}$$

Considering the relation between the center-of-mass and internal wavenumbers K and κ and the electron and hole wavenumbers k and l, see Eq B3, we find that the approach developed merely reproduces the free electron/hole pair states. A similar result is obtained when using different hopping matrix elements for the electron and the hole, see Appendix C. This outcome confirms the consistency of the proposed method of obtaining electron-hole pair states from the internal electron-hole pair Hamiltonian.

Figure 3 displays the dispersion relation $\varepsilon_{0,\kappa}$ and the corresponding density of states for the infinite chain, and for a

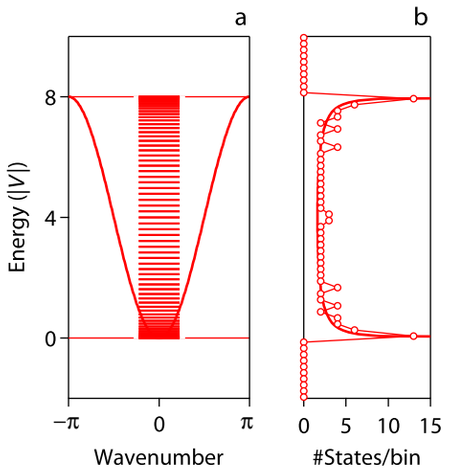

FIG. 3. Free electron-hole pair states. (a) Representation of the dispersion relation $\varepsilon_{0,\kappa}$ for the energy related to the internal state of the free electron-hole pair at $K = 0$. The horizontal lines indicate the states obtained for a $N = 128$ atom chain with periodic boundary conditions. The lowest energy of the electron-hole pair ($\varepsilon_{gap,\infty} = \varepsilon_a + \varepsilon_b - 4|V|$) is taken as the energy reference, and energies are expressed in units of $|V|$. (b) Number of internal states per energy bin $|V|/5$ for a $N = 128$ chain. The full line represents the number of states in the same energy bins for the infinite chain, calculated per $N = 128$ atoms.

$N = 128$ chain under periodic boundary conditions. Here, we took the energy of the lowest energy electron-hole pair state – the quasi-particle gap $\varepsilon_{gap,\infty}$ – as the energy reference. While providing a view on the free electron-hole pair states, the figure mostly shows that periodic boundary conditions – which preserve the translation symmetry and thus the concomitant quantum numbers – are an apt choice to model infinite chains.

B. Bound Excitons

As a second example, we take the case where the atom-localized states for which the electron and hole are co-localized on the same atom have an energy Δ lower than all other atom-localized states. Such a situation would result from a point-like attraction between the electron and the hole, as used within the Hubbard-model. This approach can be implemented in $\mathbf{H}_K$ by taking the diagonal elements as follows:

$$\varepsilon_{eh}(0) = \varepsilon_a + \varepsilon_b - \Delta \tag{17}$$

$$\varepsilon_{eh}(r) = \varepsilon_a + \varepsilon_b \text{ for } r \neq 0 \tag{18}$$

This assignment of matrix elements can be summarized by writing $\mathbf{H}_K$ as:

$$\mathbf{H}_K = \mathbf{H}_{K,kin} + \mathbf{H}_{K,int} \tag{19}$$

Here, $\mathbf{H}_{K,kin}$ is the free electron-hole Hamiltonian and $\mathbf{H}_{K,int}$ the interaction Hamiltonian, which is zero except for the diagonal element $-\Delta$ at $r = 0$. Using this separation of $\mathbf{H}_K$, we can break down the energy of each exciton state in an internal kinetic and an electron-hole interaction part. Moreover, taking the quasi-particle gap $\varepsilon_a + \varepsilon_b - 4|V|$ as the energy reference, the energy level spectrum will scale proportionally to V for a given setting of the ratio $\Delta/|V|$. Henceforth, we will therefore represent energies as reduced quantities in units of $|V|$, where the interaction energy $\Delta/|V|$ distinguishes different parameter settings.

Figures 4a-b represent the energy spectrum and the density of states of the internal electron-hole pair eigenstates, obtained by numerically solving the eigenvalue equation of the Hamiltonian at $K = 0$ and taking $\Delta/|V| = 2$ for an $N = 128$ chain with periodic boundary conditions. As can be seen, a band of energy levels is obtained that features a density of states similar to the corresponding free electron-hole pair. However, one state, denoted as $|0,\mathrm{X}\rangle$, stands out by having an energy ε_X below this band of states. Considering the expansion coefficients shown in Figure 4c, one sees that the electron-hole distance for this state is distributed in a narrow range around $r = 0$. Hence, we interpret this state as a bound electron-hole pair or exciton.

What makes the point-like electron-hole interaction interesting, is that analytical expressions exist for the eigenstates and eigenenergies of the resulting internal Hamiltonian.[17] In particular, the expansion coefficients $\psi_\mathrm{X}(r)$ and the energy ε_X of the exciton state $|0,\mathrm{X}\rangle$ can be found using the following *Ansatz*:

$$\psi_\mathrm{X}(r) = \phi_\mathrm{X}(0) e^{-\frac{|r|}{r_\mathrm{X}}} \tag{20}$$

Indeed, with this set of expansion coefficients, the eigenvalue equation of the internal Hamiltonian is reduced to a set of two equations with the energy ε_X and the characteristic length r_X as the two unknowns:

$$(\varepsilon_a + \varepsilon_b - \Delta - \varepsilon_\mathrm{X}) + 4V e^{-\frac{1}{r_\mathrm{X}}} = 0 \tag{21}$$

$$(\varepsilon_a + \varepsilon_b - \varepsilon_\mathrm{X}) + 2V\left(e^{-\frac{1}{r_\mathrm{X}}} + e^{\frac{1}{r_\mathrm{X}}}\right) = 0 \tag{22}$$

We thus obtain:

$$\varepsilon_\mathrm{X} = 4|V|\left(1 - \sqrt{1 + \frac{\Delta^2}{16V^2}}\right) \tag{23}$$

$$r_\mathrm{X} = \frac{1}{\operatorname{asinh}\left(\frac{\Delta}{4|V|}\right)} \tag{24}$$

A similar result is obtained for electron-hole pairs with different hopping matrix elements for the electron and the hole, for which $4V$ should be replaced by $2V_e + 2V_h$, see Appendix C.

Note that Eq 23 yields ε_X relative to $\varepsilon_{gap,\infty}$, i.e., the bottom of the free electron-hole pair energy band. Moreover, as predicted, the energy scales proportionally to $|V|$, while the reduced interaction energy $\Delta/|V|$ determines the exciton properties. Finally, considering the breakdown of the energy ε_X into a kinetic and an interaction energy part, one readily shows that the interaction energy $\varepsilon_{\mathrm{X},int}$ amounts to:

$$\varepsilon_{\mathrm{X},int} = \langle X,0|\,\mathbf{H}_{0,int}\,|X,0\rangle = -\Delta \tanh\left(r_\mathrm{X}^{-1}\right) \tag{25}$$

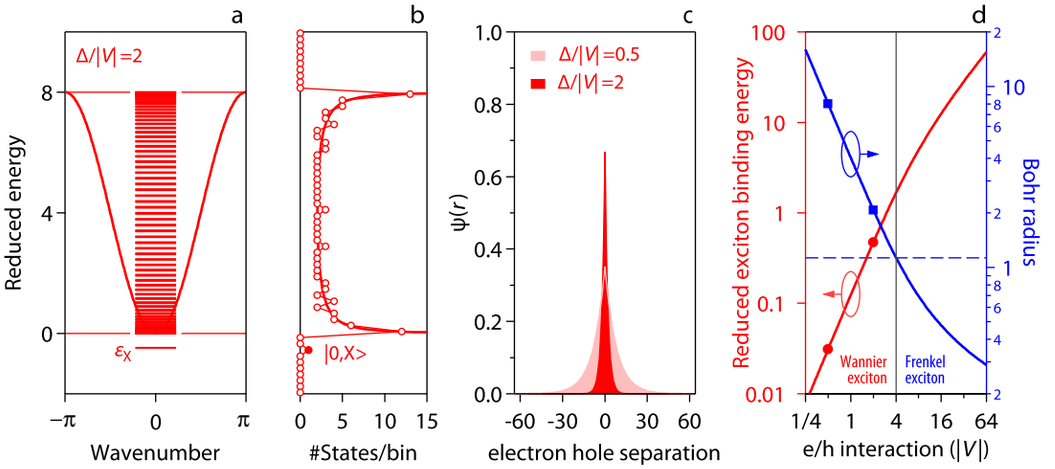

FIG. 4. Bound exciton states. (a) Reduced energy of the different eigenstates relative to the quasi-particle gap, obtained for a chain characterized by a point-like, reduced electron-hole interaction $\Delta/|V| = 2$ at $K = 0$. The calculation involved periodic boundary conditions on a $N = 128$ chain. The full line shows the dispersion of the free electron-hole pair states at $K = 0$. The bound exciton state $|0,X\rangle$ stands out as the one state with an energy ε_X below that of the free electron-hole pairs. (b) Density of states for the same system, with the full line showing the corresponding density of free electron-hole pair states. The bound exciton state is highlighted by a filled marker. (c) Expansion coefficients of the exciton state $|0,X\rangle$ as a function of r for (red) $\Delta/|V| = 2$ and (light red) $\Delta/|V| = 0.5$. (d) Variation of the binding energy ε_X and the radius r_X of $|0,X\rangle$ state as a function of the reduced electron-hole interaction energy. The markers correspond to the parameter settings used in (c).

Since the center-of-mass wavenumber is zero, the difference between ε_X and $\varepsilon_{X,int}$ can be seen as the kinetic energy related to internal motion of the bound electron-hole pair.

Figure 4d represents ε_X and r_X as a function of the reduced interaction energy $\Delta/|V|$, where the vertical line at $\Delta/|V| = 4$ delineates two regimes. In the weak-binding limit ($\Delta/|V| \ll 4$; $r_X \gg 1$), the electron and the hole can be several atoms apart, as is the case for the examples shown in Figure 4c. This spreading increases the more the electron-hole interaction is reduced. This limit agrees with what is commonly denoted as the Wannier exciton. The strong-binding limit ($\Delta/|V| \gg 4$; $r_X \ll 1$), on the other hand, is characterized by a pronounced co-localization of the electron and the hole on the same atom; a state that can be seen as a Frenkel exciton.

In the weak-binding limit, the exciton characteristics ε_X and r_X can be approximated as:

$$\varepsilon_X \approx -\frac{\Delta^2}{8|V|} \qquad r_X \approx \frac{4|V|}{\Delta} \tag{26}$$

These expressions directly show how the exciton binding energy and the exciton radius result from the trade off between delocalization – so strong coupling or low effective masses – and electron-hole interaction. Interestingly, the product $\varepsilon_X r_X^2$ boils down to $1/2|V|$. Since the reduced effective mass of the exciton amounts to $1/4|V| = m^\star/2$ – note the hopping matrix elements of $2V$ in $\mathbf{H}_0$ – this result coincides with the expected for hydrogen-like internal exciton states. We will therefore refer to r_X as the exciton Bohr radius. Moreover, as outlined in Appendix A, an electron effective mass $m^\star = 0.1$ would correspond to a hopping matrix element of 2 eV. In that case, an interaction energy $\Delta/|V| = 1/4$ would yield an exciton binding energy of ≈ 15 meV, and a Bohr radius of ≈ 16 unit cells, a typical result for tetrahedral semiconductors. In what follows, we will take this value as a reference when screening the interaction energy.

C. Exciton Center-of-Mass Motion

Similar to the $K = 0$ case, the internal Hamiltonian $\mathbf{H}_K$ at $K \neq 0$ will feature a bound exciton state. Since the coupling matrix elements scales as $2V\cos(K/2)$, the exciton energy will depend on the center-of-mass wavenumber as:

$$\varepsilon_X(K) = \varepsilon_a + \varepsilon_b - \sqrt{16V^2\cos^2\frac{K}{2} + \Delta^2} \tag{27}$$

Obviously, such a K-dependence is not unexpected if states $|K,X\rangle$ are to describe a moving exciton. However, this relation involves a combination of the kinetic energy of the center-of-mass motion and the K-dependent change of the exciton binding energy. Figure 5a represents the corresponding dispersion relation for the free electron-hole pair ($\Delta = 0$) and three selected cases of bound excitons. Clearly, the corresponding energy band $\varepsilon_X(K)$ narrows down when the interaction energy increases.

Considering the internal Hamiltonian $\mathbf{H}_K$, one sees that for small deviations of the center-of-mass wavenumber from $K = 0$, the hopping matrix element will be constant up to first order in K. Hence, wave packets with the same internal exciton state can be constructed to describe center-of-mass motion at small K, and the effective mass M of the center-of-mass can be

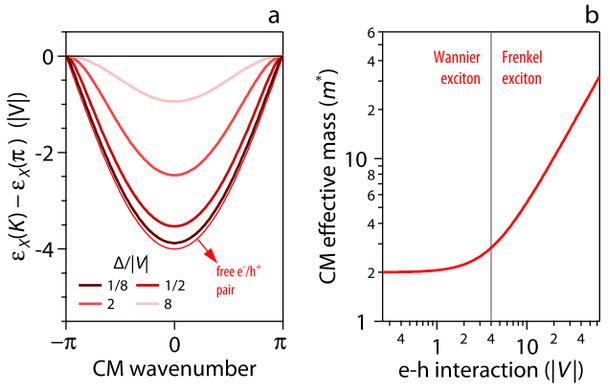

FIG. 5. Exciton center-of-mass motion. (a) Dispersion of the exciton energy as a function of the center-of-mass wavenumber, represented for selected values of the electron-hole interaction $\Delta/|V|$ as indicated. Note that each band is plotted relative to the energy attained for $K = \pi$. (b) Effective mass related to center-of-mass motion as a function of the electron-hole interaction. The vertical line indicates the separation between the weak-binding and strong-binding limits.

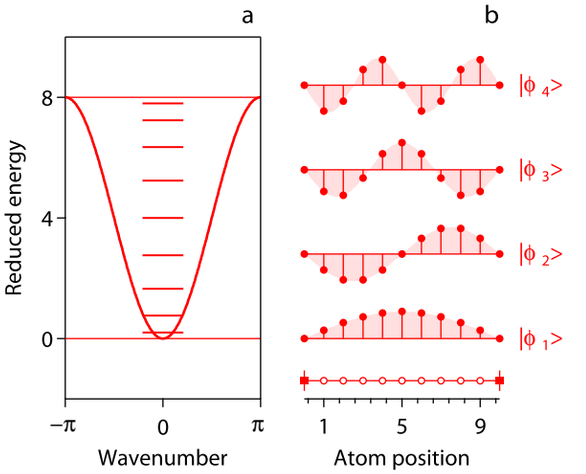

FIG. 6. Single-electron confinement. (a) Spectrum of eigenstates for an $N = 9$ chain, represented on top of the dispersion relation for the infinite chain. (b) Representation of the expansion coefficients of the four lowest-energy states on the finite chain. The lower line represents the finite chain, with open circles indicating the edge positions at $n = 0$ and $n = N+1$ where the expansion coefficients are forced to zero.

related to the inverse of the second derivative $d^2\varepsilon_X(K)/dK^2$ at $K = 0$:

$$M^\star = \frac{1}{|V|}\sqrt{1+\frac{\Delta^2}{16V^2}} = 2m^\star\sqrt{1+\frac{\Delta^2}{16V^2}} \qquad (28)$$

As shown in Figure 5b, the exciton center-of-mass features a nearly constant effective mass $M^\star = 2m^\star$, i.e., the sum of the electron and hole effective mass, in the weak binding limit. Hence, the Wannier exciton moves as a quasi-particle with a mass equal to the sum of the masses of its constituents. The strong-binding limit, on the other hand, is characterized by a pronounced increase of $M^\star$. Note that energy-transfer terms, which were not considered here, can counteract the resulting drop in mobility of Frenkel excitons.[13]

IV. EXCITONS ON FINITE CHAINS

A. From Infinite to Finite Chains

A finite, N-atom chain lacks the translational symmetry of the infinite chain. Single-electron or electron-hole pair eigenstates will therefore no longer have the symmetry-adapted from, see Eqs A3 and 9, and the eigenvalue equation of the full Hamiltonian must be solved to find the eigenstates. In this respect, the atom-localized basis provides a straightforward way of implementing infinite-well boundary conditions, by taking into account only the hopping elements to atoms within the chain for the outermost atoms – possibly using different matrix elements V_e and V_h for electron and hole hopping, respectively. Since the center-of-mass and the internal coordinate of an electron-hole pair cannot be varied independently on a finite chain – for $R = 1$, r can only be zero – the states $|a_s, b_t\rangle$ that index the position of the electron and the hole make for a more appropriate basis. However, as mentioned before, this approach raises the dimension of the Hilbert space of eigenstates to N^2.

For single-electron states, an alternative approach to find eigenstates of the N-atom chain involves forming linear combinations of degenerate eigenstates on the infinite chain, such that the expansion coefficients c_0 and c_{N+1} are zero. For such states, hopping from atom 1 or N to atom 0 or $N+1$ is ruled out, a result that implements in effect infinite-well boundary conditions.[18] In the case of a single electron, for example, the states $|k_p\rangle$ and $|-k_p\rangle$ are degenerate, and an eigenstate $|\phi_p\rangle$ of the finite chain can be obtained as:

$$|\phi_p\rangle = \tfrac{1}{\sqrt{2}}(|k_p\rangle - |-k_p\rangle)$$
$$k_p = \frac{p\pi}{N+1} \quad \text{with} \quad p = 1,2,\ldots,N \qquad (29)$$

The eigenstates $|\phi_p\rangle$ can be seen as standing waves with an increasing number of nodes along the chain, see Figure 6, where the difference between the energy of state $|\phi_1\rangle$ and the bottom of the bulk energy band yields the kinetic energy in the confined state $\varepsilon_{kin,conf}$ as:

$$\varepsilon_{kin,conf} = 4|V|\sin^2\left(\frac{\pi}{2(N+1)}\right) \approx \frac{\pi^2}{2m^\star a^2} \qquad (30)$$

This increase in kinetic energy upon confining a particle in space is typically called the confinement energy. In a first order approximation, $\varepsilon_{kin,conf}$ scales with $1/a^2$ and $1/m^\star$, a characteristic that is expected for parabolic energy bands.

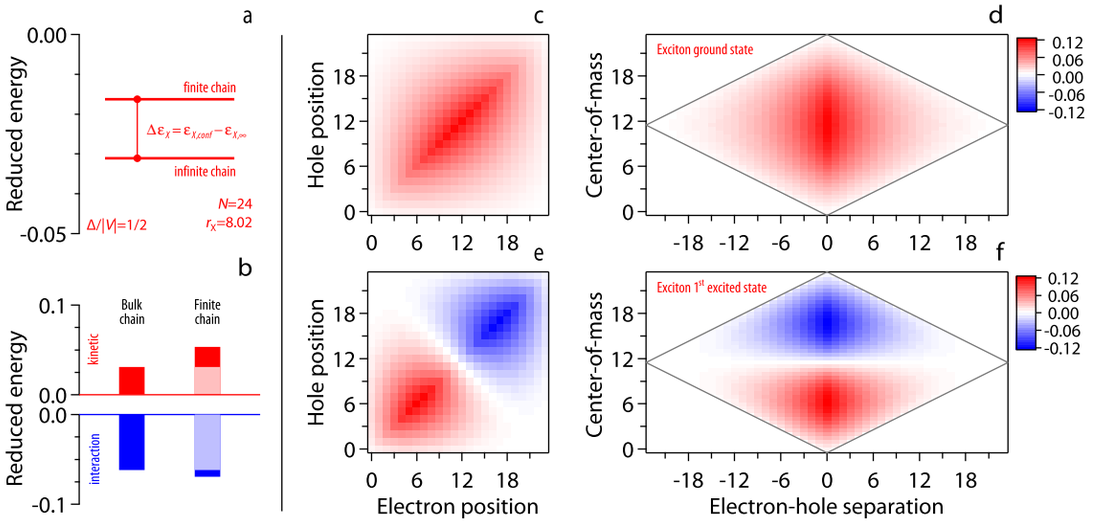

FIG. 7. Excitons in intermediate confinement. (a) Energy of the lowest exciton state determined for an $N = 24$ atom chain using the electron-hole interaction and hopping matrix element as indicated. (b) Break down of the ground state exciton energy in contributions related to (red) kinetic and (blue) interaction energy for the bulk chain and the finite $N = 24$ atom chain. (c-d) Representation of the expansion coefficient of the exciton ground state in the atom-localized electron-hole pair basis states, both as a function of the electron and hole position and the electron-hole separation and center-of-mass coordinates. (e-f) The same for the first excited exciton state.

B. The Strong Confinement Reference

Strong confinement refers to the regime in which the confinement energy is the dominant energy term, which makes the finite chain hosting a free electron-hole pair the reference system to describe this regime.[3,19] In that case, the boundary conditions require that both the electron and hole eigenstates have expansion coefficients vanishing at $n = 0$ and $n = N+1$. As a result, the ground state of the electron/hole pair will exhibit an energy increase ε_{SQ} as given by:

$$\varepsilon_{SQ} = 8|V|\sin^2\left(\frac{\pi}{2a}\right) \approx \frac{\pi^2}{2\mu^\star a^2} \tag{31}$$

Here, $\mu^\star = m^\star/2$ is the reduced mass of the electron-hole pair. Given the absence of any electron-hole interaction, ε_{SQ} can be attributed entirely to a kinetic energy change, i.e., the confinement energy. In particular, the first order approximation in Eq 31 is the 1D equivalent of the confinement energy in the expression proposed by Brus, see Eq 1.

C. The Weak Confinement Reference

Weak quantization corresponds to the limit in which the Bohr radius of the bound exciton is considerably smaller than the length of the chain.[3] In this regime, the boundary conditions can be implemented in good approximation by applying the procedure for single-particle states to the center-of-mass motion of the exciton, thereby restricting K to multiples of $\pi/(N+1)$. Considering the dispersion relation for the center-of-mass motion of the bound exciton, Eq 27, we thus obtain an increase $\Delta\varepsilon_X$ of the exciton energy of:

$$\Delta\varepsilon_X \approx \frac{1}{2\sqrt{1+\frac{\Delta^2}{V^2}}}\frac{\pi^2}{M^\star a^2} \tag{32}$$

Here, $M^\star = 2m^\star$ is the total mass of the electron-hole pair. Hence, also in the weak quantization limit, we find that the increase of the exciton energy scales in proportion to $1/a^2$.[3] Moreover, in the case of Wannier excitons, the coefficient relating the quantization energy and $1/a^2$ will be a quarter of that in the strong quantization limit, a difference reflecting the ratio between the effective mass $M^\star$ of center-of-mass motion and the reduced effective mass $\mu^\star$ of the electron-hole pair. In that case, $\Delta\varepsilon_X$ can be interpreted as ε_{WQ}, i.e., the additional kinetic energy of the exciton in the weak confinement limit:

$$\varepsilon_{WQ} = 2|V|\sin^2\left(\frac{\pi}{2a}\right) \approx \frac{\pi^2}{2M^\star a^2} \tag{33}$$

For the Frenkel exciton, on the other hand, $\Delta\varepsilon_X$ will be a combination of a change in kinetic and interaction energy.

D. Excitons in Intermediate Confinement

Within the basis of atom-localized electron-hole pair states $|a_s, b_t\rangle$, the Hamiltonian matrix can be constructed for any chain length and any electron-hole interaction $\Delta/|V|$. Similar to the internal Hamiltonian, see Eq 19, the resulting operator can be split into a kinetic and an interaction energy part:

$$\mathbf{H} = \mathbf{H}_{kin} + \mathbf{H}_{int} \tag{34}$$

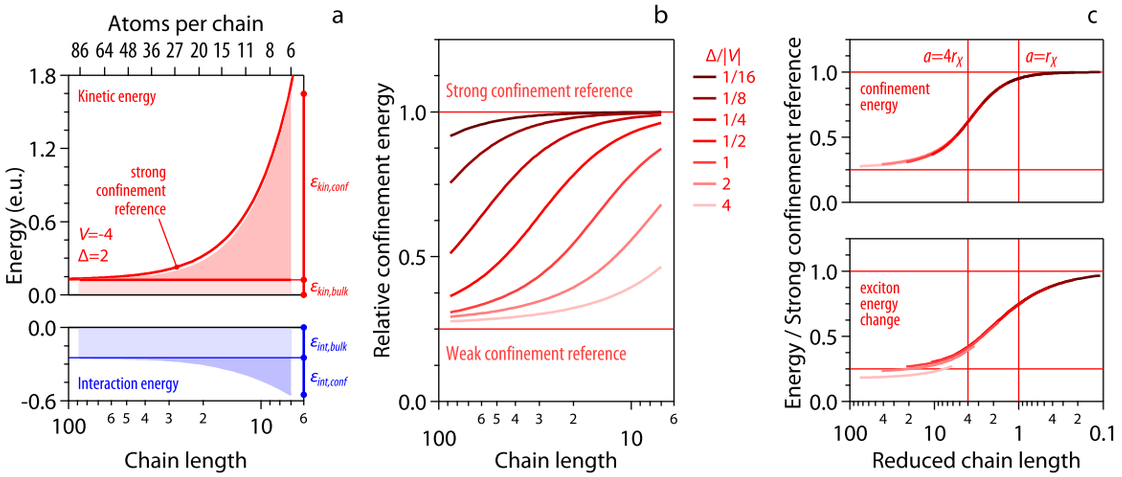

FIG. 8. Transition from weak to strong confinement. (a) Variation of (filled red) the kinetic energy and (filled blue) the interaction energy of the exciton ground state as a function of the atom chain length. Light colors represent the bulk contributions to both energies, dark colors the additional energy for the confined exciton on a finite chain. Parameter settings were taken as indicated. (b) Variation of the ratio between the kinetic energy of confinement and the strong confinement reference for different electron-hole interaction energies. The limits for weak and strong confinement have been indicated. (c) Representation of (top) the relative confinement energy and (bottom) the relative exciton energy change obtained for different interaction energies as a function of the reduced chain length, i.e., the chain length in units of the Bohr radius. In particular for the relative confinement energy, a nearly unique relation is obtained. For the exciton energy changes, deviations from a unique relation are visible for the $\Delta/|V| = 2$ and $\Delta/|V| = 4$, settings that approach the Frenkel excitons.

Factorizing out the hopping energy V, one sees that also in this case, the ratio Δ/V will be the defining parameter for the Hamiltonian. Moreover, exciton eigenstates can be obtained by numerically solving the eigenvalue equation of $\mathbf{H}$, without resorting *a priori* to the limit of strong or weak confinement. Figure 7a represents, for example, the energy calculated for the exciton ground state on a $N = 24$ chain with an interaction energy $\Delta/|V| = 1/2$. For this interaction energy, $r_X \approx 8$, which means that the length of the chain is about three times the Bohr radius r_X. As can be seen in Figure 7a, the energy of the exciton ground state on this chain indeed exceeds that for the infinite chain. In line with the relation proposed by Brus,[2] Figure 7b displays the breakdown of ε_X into a kinetic and an interaction energy part. For the bulk exciton, the interaction energy is about twice the kinetic energy of the exciton – the same ratio as for the hydrogen atom ground state. Reducing the chain length, however, raises the kinetic energy more than the interaction energy, which leads to the resulting net increase of the exciton energy upon size reduction.

Figures 7c-d display the expansion coefficients of the exciton ground state in the atom-localized basis using the electron and hole position, and the center-of-mass and the internal coordinate, respectively. In line with the parameter settings yielding $r_X \approx 8$, the states where $r = 0$ – so $s = t$ – feature the largest expansion coefficients. On the other hand, the finite chain length imposes a sine-like modulation of the expansion coefficients along the center-of-mass coordinate, whereas the spread of the exciton wavefunction at fixed R is clearly restricted close to the chain edge. In addition, Figures 7e-f give a similar representation of the expansion coefficients of the first excited state. In agreement with the discussion of weak quantization, this state consists approximately of the bound exciton state, but modulated as a first overtone by a sine-like envelope whose wavelength matches the full length rather than half the length of the chain.

E. The Transition from Weak to Strong Confinement

Taking the chain length as an adjustable parameter, we can systematically track the change in the exciton energy, and the breakdown of this energy change in a kinetic and interaction part, for a given setting of the hopping and interaction energy. Figure 8a displays the result of this exercise using the same parameter setting as in Figure 7, i.e., $\Delta/|V| = 1/2$. As can be seen, the kinetic energy becomes the dominant contribution to the exciton energy upon size reduction. Moreover, the change in kinetic energy approaches the strong confinement reference with decreasing size; the central assumption of the Brus equation. To better evaluate the impact of size reduction, Figure 8b displays the ratio between the calculated change in kinetic energy, and the change expected in the limit of strong confinement. This relative confinement energy indeed levels off at 0.25 – the weak confinement limit – for long chains and a strong electron-hole interaction, and approaches 1 – the strong confinement limit – in the case of short chains and a weak electron-hole interaction. Focusing on the $\Delta/|V| = 1/2$ case – for which $r_X \approx 8$ – one sees that the shift between both limits takes about a 10-fold reduction of the chain length.

Interestingly, the traces obtained for different electron-hole interaction energies as shown in Figure 8b appear as shifted copies of a single, underlying relation between the relative

confinement energy and the chain length. Figure 8c shows that such a nearly unique relation is indeed obtained when considering the reduced chain length $a_{red} = a/r_X$, i.e., the chain length in units of the Bohr radius, as the independent variable. From this relation, it follows that the confinement energy is halfway the weak and strong confinement limit for $a_{red} = 4$ and attains 95% of the strong confinement reference when $a_{red} = 1$. Clearly, this result highlights the relevance of the Bohr radius – as proposed by Brus – as an upper limit of strong quantization. Moreover, leaving aside the cases of the highest electron-hole interaction that yield Frenkel excitons, also the combination of the confinement energy and the change in interaction energy yields a relative exciton energy shift that is a nearly unique function of the reduced chain length, see Figure 8c. Not unlike the sizing curve in the strong confinement regime,[20] this observation suggests that also the transition from weak to strong confinement could be described using a generic sizing curve.

F. Confinement and Charge-Carrier Delocalization

Figure 9a-c displays the expansion coefficients of the exciton ground state on a finite chain, for a progressively smaller electron-hole interaction. One sees that this variation comes with a transition from a state where the electron and hole remain in close proximity and the center-of-mass is delocalized along the entire chain, to a state where the electron and hole delocalize both as independent particles. The latter state closely resembles the lowest energy state of the non-interacting electron-hole pair shown in Figure 9d. This change in delocalization regime can be quantified using the participation fraction f, which we define for a given eigenstate as:

$$f = \frac{1}{N^2} \times \frac{1}{\sum_{s,t} c_{s,t}^4} \tag{35}$$

Here, $c_{s,t}$ is the normalized expansion coefficient for the basis state $|a_s, b_t\rangle$. By normalizing to the number of basis states, f can be interpreted as the fraction of the basis states that contribute to a given eigenstate. A state localized on a single pair of atoms, will show a participation fraction of $1/N^2$, while f will scale proportional to $1/N$ for states delocalized along one coordinate – such as the center-of-mass – and states with equal contributions from all basis states will have $f = 1$.

Figure 9e displays the participation fraction as a function of the chain length, for different settings of the electron-hole interaction. Taking the scaling references, one sees that the weak confinement regime, i.e., long chains and strong electron-hole interaction, is indeed characterized by a participation fraction scaling as N^{-1}, which reflects the delocalization of the center-of-mass. For short chains and weak electron-hole interaction, however, a nearly constant participation fraction is obtained that coincides with the expected for the confined free electron-hole pair. Importantly, this transition again occurs for chain lengths comparable to the exciton Bohr radius. This point underscores that the full delocalization of the electron and the hole is a second defining feature of

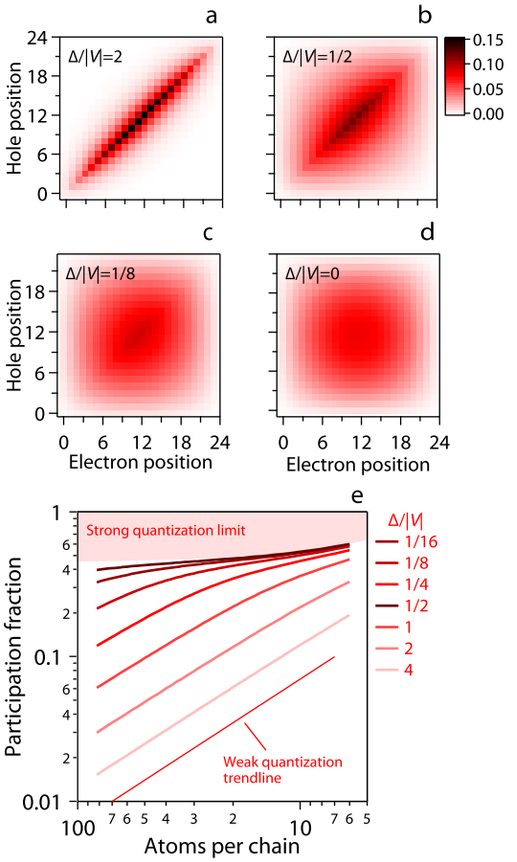

FIG. 9. Confinement and delocalization. (a-d) Representation of the expansion coefficients of the confined exciton ground state in the localized electron-hole pair basis for a decreasing electron-hole interaction as indicated. The same color coding is used throughout. (e) Participation fraction as a function of the number of atoms per chain. The filled background represents the limit for strong quantization of non-interacting electron-hole pairs, while the thin red line displays the trend line expected for weak quantization.

the strong quantization limit, next to an energy change dominated by the confinement energy.

V. DEFECT-LOCALIZATION AND CONFINEMENT

A. Single Electron Localization by Defects

Until now, we considered exciton states on an infinite chain that is invariant under a translation by a lattice vector, or finite chains that are simply a shortened version of this perfect infinite chain. In the case of electron/hole pairs, the eigenstates of such chains are either running waves on infinite, and delocalized confined states on finite chains – in terms of the center-of-mass in the case of weak confinenemt and of the separate charge carriers in the case of strong confinement. In real chains, however, the position of an atom can deviate from the

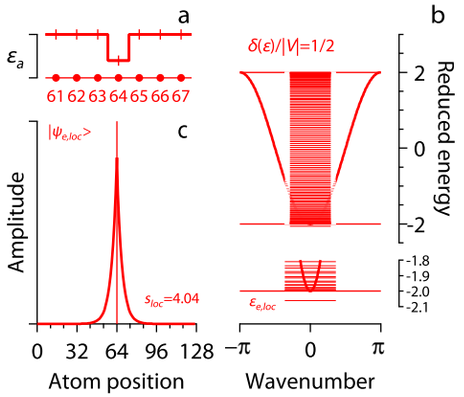

FIG. 10. Single electron localization (a) Representation of a point defect where the on-site energy on a single atom is lower than on all other atoms. (b) Energy level spectrum calculated for an $N = 128$ atom chain with periodic boundary conditions using a lower energy on atom $s = 64$ as indicated. The bottom inset provides a zoom on the low-energy edge, showing the formation of a state with energy $\varepsilon_{loc,e}$ below the band of delocalized states. (c) Expansion coefficients of the single-electron ground state $|\psi_{e,loc}\rangle$, underscoring the localization of the electron around the defect, with a characteristic localization length s_{loc}.

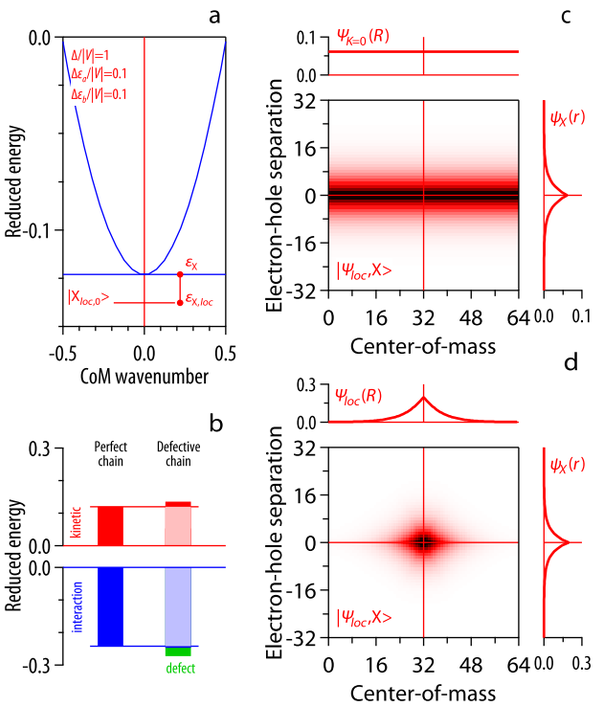

FIG. 11. Exciton localization. (a) Representation of (red) the lowest energy state of a defective atom chain, for which the on-site electron and hole energy are reduced on one atom as indicated and (blue) the dispersion relation for center-of-mass motion of the bound exciton on the perfect chain. (b) The break down of the energy of the exciton ground state in terms of kinetic, interaction and defect-localization energy. One sees that localization hardly changes the electron-hole interaction energy. (c-d) Representation of the expansion coefficients as a function of the center-of-mass and internal coordinates for the exciton ground state on the (c) perfect and (d) defective chain. The side curves represent the variation of the expansion coefficients as a function of R and r, respectively. Calculations done using periodic boundary conditions, where the defective atomic site is placed in the center of the chain.

perfect lattice points. Such defects break translational symmetry, thereby affecting the properties of the eigenstates on the bulk chain and the way these states change when chains are made shorter.

In the case of a single electron, analytical expressions for the eigenstates can be found in cases where a single atom in the chain has a different on-site energy – which would represent a substitutional point defect – or where a single pair of atoms exhibits a different hopping matrix element. As outlined in Appendix D, such defects lead to a lowest energy eigenstate $|\psi_{e,loc}\rangle$ that is no longer delocalized across the entire crystal, but localized around the defect. As illustrated in Figure 10, the expansion coefficients of this state in the atom-localized basis drop exponentially with the distance from the point defect. The state $|\psi_{e,loc}\rangle$ can therefore be characterized by a localization length s_{loc}, which is the characteristic decay length of these expansion coefficients. As shown in Appendix D, s_{loc} will be shorter, and the defect-localization energy $\varepsilon_{e,loc}$ larger, for stronger deviations from the lattice periodicity; while a larger hopping matrix element – so lower effective masses – limits the impact of localization.

B. Exciton Localization by Defects

According to Eq 15, describing the interacting electon/hole pair by means of a center-of-mass and an internal coordinate yields a Hamiltonian matrix $\mathbf{H}_K$ from which the internal states can be obtained for a given center-of-mass wavevector K. Importantly, one sees that for small K, $\mathbf{H}_K$ is constant up to first order in K. Therefore, minor defects will mostly lead to a localization of the center-of-mass, by creating eigenstates $|\mathrm{L,X}\rangle$ that are a superposition of exciton eigenstates $|K,\mathrm{X}\rangle$ with different K but the same internal exciton state $|\mathrm{X}\rangle$:

$$|\mathrm{L,X}\rangle = \sum_K \sum_R \Phi_\mathrm{L}(K) e^{iKR} \left(\sum_r \psi_\mathrm{X}(r) | a_{R+\frac{r}{2}}, b_{R-\frac{r}{2}} \rangle \right)$$
$$= \sum_R \Psi_\mathrm{L}(R) \left(\sum_r \psi_\mathrm{X}(r) | a_{R+\frac{r}{2}}, b_{R-\frac{r}{2}} \rangle \right) \quad (36)$$

Here, $\Phi_\mathrm{L}(K)$ and $\Psi_\mathrm{L}(R)$ are introduced as the expansion coefficients of the center-of-mass state in the plane-wave and atom-localized basis, respectively. Note that $\Psi_\mathrm{L}(R)$ therefore describes the spread of the eigenstate $|\mathrm{L,X}\rangle$ along the center-of-mass coordinate.

The approximate description of exciton localization as impacting only the center-of-mass coordinate is illustrated in Figure 11. Here, Figure 11a displays the lowest energy state for a chain containing one atom with reduced on-site energies ε_a and ε_b, in comparison with the dispersion relation of

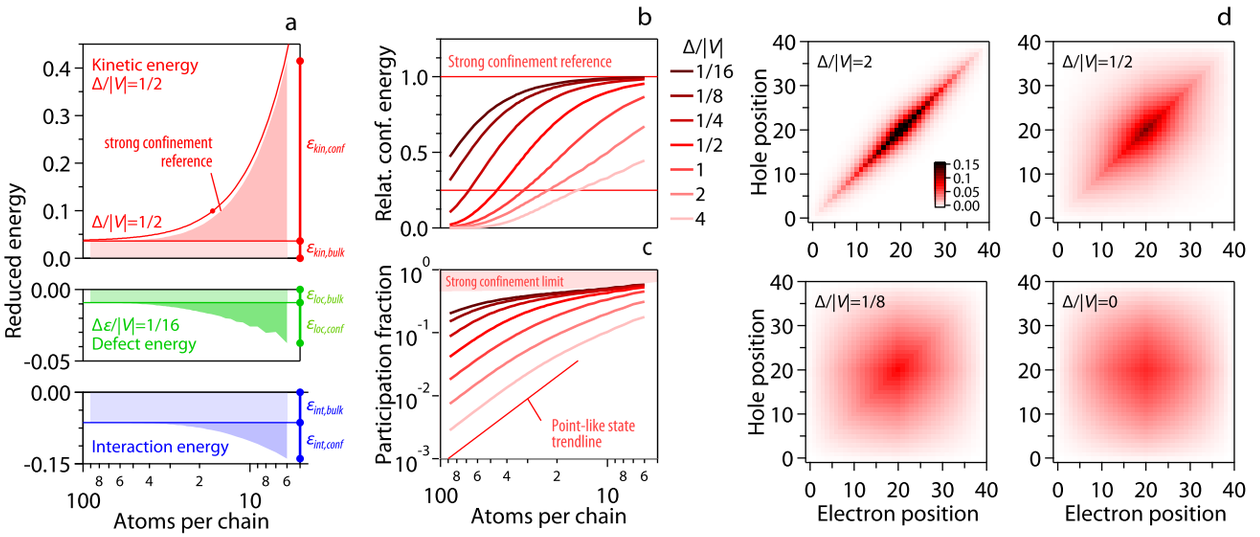

FIG. 12. Confinement of localized excitons. (a) Breakdown of the energy of the localized exciton ground state in contributions of (red) kinetic, (green) localization and (blue) interaction energy as a function of the chain length. Parameter settings as indicated. The energy reduction refers to a change of the on-site electron and hole energy of the atom in the center of the chain. (b-c) Relative confinement energy and participation fraction as a function of chain length, for different electron-hole interaction energies as indicated. (d-g) Representation of the localized exciton ground state for an $N = 40$ atom chain for decreasing electron-hole interaction as indicated. The same defect is used for all simulations shown.

the bound excitons on the perfect chain. Similar to the single particle case, a reduction of the on-site energy leads to an exciton eigenstate with an energy lower than the $|0,\mathrm{X}\rangle$ state. In Figure 11b, the energy of this eigenstate is broken down in a kinetic, interaction and defect contribution, which is accomplished by writing the Hamiltonian as (see also Eq 34):

$$\mathbf{H} = \mathbf{H}_{kin} + \mathbf{H}_{int} + \mathbf{H}_{def} \tag{37}$$

Here, $\mathbf{H}_{def}$ contains all deviations from the perfect chain – in this case the lowering of ε_a and ε_b for a single atom. Moreover, by factorizing out the hopping energy V, one sees that the parameters defining the Hamiltonian are now the reduced interaction energy $\Delta/|V|$, and the reduced defect energy, such as the on-site terms $\delta(\varepsilon_a)/|V|$ and $\delta(\varepsilon_b)/|V|$

As can be seen in Figure 11b, a point defect such as a variation of the on-site energy changes the energy of the lowest exciton state through the combination of a negative defect-localization energy that is partially compensated by an increased kinetic energy. The interaction energy, on the other hand, is mostly unchanged. This result confirms the interpretation that defects mostly induce a localization of the center-of-mass around the defect, in which case the electron-hole interaction would remain unchanged and the additional kinetic energy reflects the localization of the center-of-mass around the defect. This conclusion is illustrated further in Figure 11c-d, where the expansion coefficients of the lowest energy exciton state are shown on a perfect and a defective chain. A comparison of the expansion coefficients as a function of R for $r = 0$ – shown on top of each graph – highlight the transition from a delocalized to a localized center-of-mass induced by the defect. On the other hand, the variation of the expansion coefficients as a function of r at fixed R hardly changes upon introduction of the defect.

C. Confinement of Localized Excitons

Using the Hamiltonian expressed by Eq 37, exciton eigenstates can be calculated as a function of the length of a given chain. Figure 12a displays the breakdown of the exciton ground state energy in a kinetic, interaction and defect contribution for a finite chain where the central atom has the on-site energies lowered by $\delta(\varepsilon_a)/|V| = \delta(\varepsilon_b)/|V| = 1/16$. For the interaction energy considered, such a defect yields a center-of-mass localization length $r_{loc} \approx 10$. As a result, the exciton ground state on a long chain features, next to a non-zero kinetic and interaction energy, also a given defect-localization energy. With decreasing chain length, the interaction and defect-localization energy become more negative – the latter reflecting the increasing weight of the confined exciton state on the defect site. However, this energy reduction is outpaced by the increase of the confinement energy, which again becomes the dominant energy contribution in the limit of short chains and weak electron-hole interaction.

To better track the size dependence of the confinement energy, Figure 11b represents the relative confinement energy as a function of the chain length. In line with the Brus equation, one sees that excitons with a weak electron-hole interaction on short chains, still evolve towards the strong-confinement limit, even if localization makes that the deviation from strong confinement is more pronounced with increasing chain length. On the other hand, for strongly bound excitons on long chains,

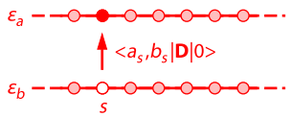

FIG. 13. Representation of optical excitations as related to the formation of electron-hole pairs on the same atom.

the relative confinement energy no longer levels off at the weak confinement limit. Rather, the confinement energy vanishes entirely. This trend reflects the formation of exciton states localized around a defect site. As soon as the Bohr radius and the center-of-mass localization length are considerably smaller than the chain length, these states no longer experience any influence from the chain boundaries. This point is confirmed by the participation fraction, which features the N^{-2} dependence characteristic for localized, point-like states for excitons with high interaction energy on large chains. Hence, while localization makes that the transition to strong confinement only occurs at a shorter chain lengths for a given electron-hole interaction energy, the weak confinement regime is undone by defect-related exciton localization.

Figure 11d-g illustrates this conclusion by means of the localized exciton ground state for $N = 40$ chains with a point defect on atom 20. In particular for the largest interaction energy, one sees that the center-of-mass localization keeps the exciton centered within the chain, such that neither the internal coordinate nor the center-of-mass coordinate really extend to the chain edges. This situation still exemplifies a point-like exciton state, which only changes little with varying chain length. Figures 11e-g illustrate the gradual transition towards a delocalized free electron-hole pair when the electron-hole interaction is decreased, although even for $\Delta/|V| = 0$, the imprint of the on-site defect on the electron-hole pair eigenstate can still be discerned.

VI. LIGHT ABSORPTION BY CONFINED EXCITONS

A. The Dipole Operator

Upon absorption of a photon, the atomic chain makes a transition from the ground state $|0\rangle$ to an electron-hole pair eigenstate $|n\rangle$, where n would be the combination of a center-of-mass wavenumber K and an internal quantum number ν for eigenstates on an infinite chain. The transition rate W between both states is proportional to the square of the transition dipole moment $D_{n;0}$, which is the matrix element of the dipole operator $\mathbf{D}$:

$$D_{n;0} = \langle n|\mathbf{D}|0\rangle = \sum_{s,t} c_{n,st}\langle a_s, b_t|\mathbf{D}|0\rangle \tag{38}$$

A straightforward way to make the dipole operator more concrete, is by considering the electron-hole pair states in the atom-localized basis that we used in the above equation for expanding $|n\rangle$. Here, the most significant transition dipole moments will be obtained for states $|a_s, b_s\rangle$ where the electron and the hole are found on the same atom, see Figure 13.[15] These are, in fact, transitions between the atomic orbitals on the same atom, which is the usual situation for interband transitions in semiconductors. When neglecting transitions between neighboring atoms and writing the transition dipole moment $\langle a_s, b_s|\mathbf{D}|0\rangle$ as d_0, $\mathbf{D}$ can be written as:

$$\mathbf{D} = d_0 \sum_s |a_s, b_s\rangle\langle 0| \tag{39}$$

Note that in this expression, we limit $\mathbf{D}$ to the part responsible for light absorption, and omit contributions that would yield stimulated emission. For a given eigenstate $|n\rangle$, D_{n0} is then obtained as the sum of the expansion coefficients of all basis states $|a_s, b_s\rangle$:

$$D_{n;0} = d_0 \sum_s c_{n,ss} \tag{40}$$

As outlined in Appendix E, a sum rule applies, stating that the sum of the squares of the transition dipole moments over all eigenstatets $|n\rangle$ will always equal the number of atoms in a given chain:

$$\sum_n D^2_{n;0} = N d_0^2 \tag{41}$$

B. Transition Dipole Moments for States on Infinite Chains

1. Free Electron-Hole Pair States

The eigenstates of the free electron-hole pair are running waves characterized by electron and a hole wavenumbers k and l, respectively. Considering an N-atom chain with periodic boundary conditions, the expansion coefficients of these states in the atom-localized basis read:

$$c_{kl,st} = \frac{1}{N} e^{i(ks+lt)} \tag{42}$$

Hence, the transition dipole moment $D_{(kl)0}$ is obtained as:

$$D_{(k,l);0} = \frac{d_0}{N}\sum_s e^{i(ks+ls)} = \frac{d_0}{N}\sum_R e^{i(k+l)R} \tag{43}$$

As outlined by the second part of this relation, the transition dipole moment is obtained as the sum over the center-of-mass coordinate of all $r = 0$ expansion coefficients for a given electron-hole eigenstate. Since k and l will be integer multiples of $2\pi/N$, $D_{(kl);0}$ will therefore be zero unless $l = -k$. We thus retrieve the familiar selection rule that only transitions between valence- and conduction-band states that preserve the electron wavenumber – or that keep the center-of-mass wavenumber K at zero – are allowed. Moreover, for such transitions, $D^2_{(kl)0}$ is a fixed number, independent of the chain length N:

$$D^2_{(k,-k);0} = d_0^2 \tag{44}$$

Note that a chain will have N bright free electron-hole pair eigenstates, so this result for $D^2_{(k,-k);0}$ aligns with the sum rule given by Eq 41.

2. Bound Excitons

The bound exciton eigenstates $|K,\nu\rangle$ are most conveniently written in the atom localized basis characterized by the center-of-mass coordinate R and the internal coordinate r:

$$|K,\nu\rangle = \frac{1}{\sqrt{N}}\sum_R e^{iKR}\sum_r \psi_{\nu,K}(r)|a_{R+\frac{r}{2}}b_{R-\frac{r}{2}}\rangle \tag{45}$$

For every center-of-mass position R, only the state for $r=0$ – for which the electron and the hole are on the same atom – will contribute to the transition dipole moment. We thus have:

$$D_{(K,\nu);0} = \frac{d_0}{\sqrt{N}}\sum_R e^{iKR}\psi_{K,\nu}(0) \tag{46}$$

Hence, the transition dipole moment is obtained as the sum of the expansion coefficients at $r=0$ for all center-of-mass positions. As shown in Figure 14a-b, these expansion coefficients add up coherently when $K=0$, while they will cancel in pairs once $K\neq 0$. Therefore, we again reach to conclusion that only $K=0$ states will be optically active, for which the square of the transition dipole moment is obtained as:

$$D^2_{(0,\nu);0} = Nd_0^2\psi_{0,\nu}(0)^2 \tag{47}$$

Since the expansion coefficients $\psi_{0,\nu}(0)$ are normalized, we again find a result in agreement with the sum rule for $D^2_{(0,\nu);0}$.

Note that according to Eq 47, the square of the transition dipole moment for the formation of, for example, the bound exciton $|\mathrm{X},0\rangle$ will scale proportionally to the number of atoms in the chain. This is a known result,[21] which contrasts with transitions involving free electron/hole pairs, and is brought about by the delocalization of the center-of-mass of the bound exciton, for which all atomic transition dipole moments contribute in phase when $K=0$. The scaling of the transition probability with N forms the basis of the so-called giant oscillator strength of the bound exciton – a situation we will denote here as the giant transition dipole moment. Using the analytical expression for the bound exciton wavefunction ψ_{X}, the square of the transition dipole moment can be rewritten in terms of the exciton Bohr radius as:

$$D^2_{(0,\nu);0} = Nd_0^2\tanh\left(\frac{1}{r_{\mathrm{X}}}\right) \tag{48}$$

Hence, the smaller r_{X}, the more significant the transition dipole moment of the bound exciton.

3. Localized Excitons

Using the approximate description that a defect mostly leads to center-of-mass localization, see Eq 36, the transition dipole moment of the localized exciton can be written as:

$$D^2_{(\mathrm{L,X});0} = \left(\sum_R \Psi_{\mathrm{L}}(R)\right)^2 d_0^2\psi_{0,\nu}(0)^2 \tag{49}$$

Hence, opposite from the delocalized exciton, we find that localized excitons have a fixed transition dipole moment, independent of the number of atoms in the chain. In fact, the scaling with N is replaced by a proportionality with $(\sum_R \Psi_{\mathrm{L}}(R))^2$. To better grasp the meaning of this prefactor, let us assume $\Psi_{\mathrm{L}}(R)$ exhibits an exponential decay away from the defect, with a characteristic localization length R_{loc}. Assuming $R_{loc}\gg 1$, one shows that:

$$\left(\sum_R \Psi_{\mathrm{L}}(R)\right)^2 = 4R_{loc} = N_{coh} \tag{50}$$

Hence, $(\sum_R \Psi_{\mathrm{L}}(R))^2$ is a measure of the spatial extension of the center-of-mass wavefunction $\Psi_{\mathrm{L}}(R)$. Typically, this quantity is referred to as the coherence length – in the units adopted here the coherence number – N_{coh}, which provides the number of atoms that coherently add their transition dipole moment to obtain the overall transition dipole moment of the localized exciton. Obviously, one has:

$$D^2_{(\mathrm{L,X});0} = \frac{N_{coh}}{N}D^2_{(0,\mathrm{X});0} \tag{51}$$

Note that this relation can also be seen as defining the coherence length.[22]

C. Transition Dipole Moments for States on Finite Chains

By means of these reference models on infinite chains, one can analyze the evolution of the transition dipole moment upon reducing the chain length. Here, we again calculated the eigenstates and eigenenergies by omitting the hopping matrix elements to atoms outside of the chain, and obtained the transition dipole moment as a sum of the $r=0$ expansion coefficients, as outlined in Eq 40. Focusing first on perfect chains, Figure 15a shows that the in the regime of weak confinement, i.e., long chains with strong electron-hole interaction, the square of the transition dipole moment scales with the chain length, in agreement with the expected for the giant transition dipole moment of the delocalized bound exciton. On the other hand, the shift to strong confinement, i.e., short chains with weak electron-hole interaction, makes the transition dipole moment level off at that of the delocalized free electron-hole pair, which serves as a lower limit to the transition dipole moment.

Figure 15b displays the transition dipole moment obtained through a similar procedure for excitons confined on a defective chain, where we implemented the same on-site defect in the chain center as in Figure 12. In line with the conclusion that such defects do not significantly alter the strong confinement behaviour, one sees that in the limit of short chains and weak electron-hole interaction, the transition dipole moment still concurs with the expected for the free electron/hole pair. In the weak confinement limit, on the other hand, the presence of a defect breaks the development of the giant transition dipole moment. Rather than systematically increasing with the number of atoms in the chain, one sees that the square

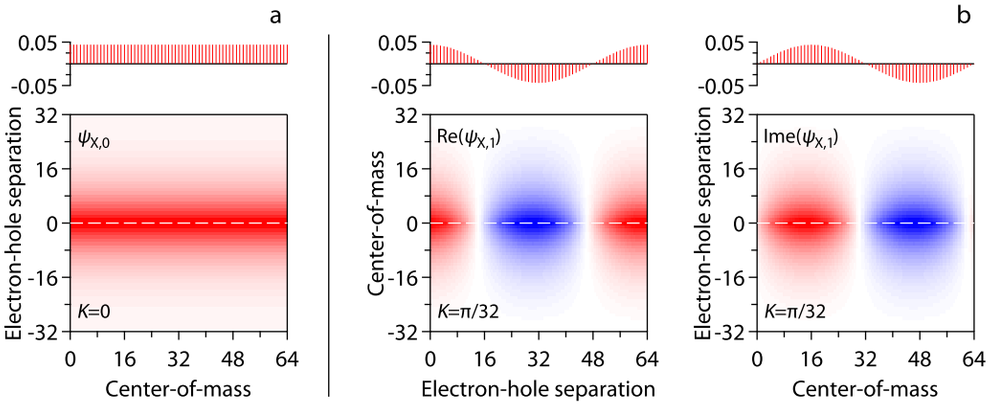

FIG. 14. Transition dipole moment for exciton states. (a) Representation of expansion coefficient of the bound exciton state at $K = 0$ in the atom-localized basis. The diagram on top displays the coefficients $\psi_{K,0}(0)$ for $r = 0$ as a function of R. (b) Representation of the real and imaginary parts of the expansion coefficient of the bound exciton state at $K = \pi/32$, and the expansion coefficients $\psi_{K,0}(0)$ as a function of R. Calculations done for a $N = 64$ chain with periodic boundary conditions using $\Delta/|V| = 1/2$.

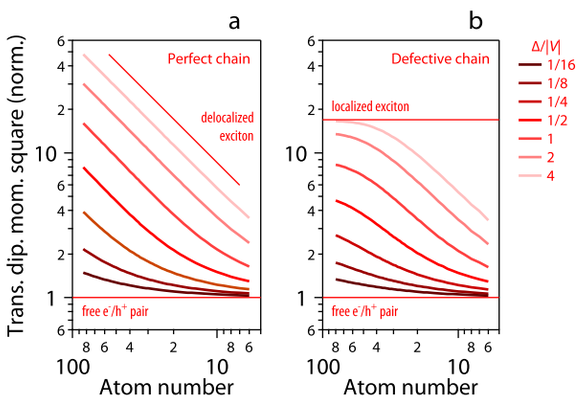

FIG. 15. Transition dipole moment for confined excitons. (a) Representation of the square of the transition dipole moment for an exciton confined on a perfect chain, for different interaction energies as indicated. The limiting cases of the free electron-hole pair and the bound exciton on an infinite chain have been indicated. (b) The same for an exciton confined on a defective chain, featuring a reduced on-site energy $\Delta(\varepsilon)/|V| = 1/16$ for the electron and hole in the center of the chain. The limiting cases of the free electron-hole pair and the bound exciton on an infinite chain for $\Delta/|V| = 1/16$ have been indicated.

of the transition dipole moment levels off at a fixed value, which coincides with the expected for the localized exciton on an infinite chain featuring the same point defect. Hence, while the regime of strong confinement appears quite robust against crystal defects, deviations from the ideal chain can have a strong effect on the energy and the transition dipole moments of the exciton states in the regime of weak confinement, thereby eliminating for example the giant transition dipole moment of the delocalized exciton.

VII. CONCLUSIONS

We used a two-particle, 1D Hubbard model to describe the impact of size reduction on the eigenstates and energy levels of electron/hole pairs in a semiconductors. Using the free electron/hole pair, and the bound exciton as reference states, the gradual transition from weak to strong confinement can be tracked as a function of the electron/hole interaction. We show that states in strong confinement approach those of the free electron/hole pair, for which the confinement energy dominates and the electron and the hole fully delocalize across the chain. States in weak confinement, on the other hand, approach exciton center-of-mass standing waves, for which only the center-of-mass delocalizes across the chain. Moreover, by introducing point defects, we demonstrate that mostly in the weak confinement regime, localized exciton states are obtained that are unaffected by size quantization once the chain length is considerably larger than the localization length. Moreover, we provide the transition dipole moment for these different reference states – free electron/hole pair, delocalized and localized exciton – and show that the transition to weak confinement comes with the development of a giant transition dipole moment, which is again capped at a fixed value for excitons on a defective chain. Rooted in the existing theory of the Hubbard model, this 1D chain can be further adapted to explore different aspects of size quantization, in relation to the properties of a given semiconductor, or specific quasi particles, such as trions or biexcitons.

ACKNOWLEDGMENTS

Z.H. acknowledges the FWO-Vlaanderen (projects G0B2921N and G0C5723N) and Ghent University (01G02124)) for research funding.

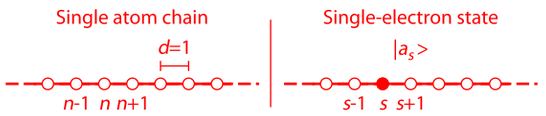

FIG. 16. (a) Representation of the chain of atoms, where each atom is identified by the running label $n = \{\ldots,-1,0,1,\ldots\}$ and the lattice parameter is taken as 1. (b) Representation of the single-electron state $|a_s\rangle$, which corresponds to a state where a single electron is localized on atom s.

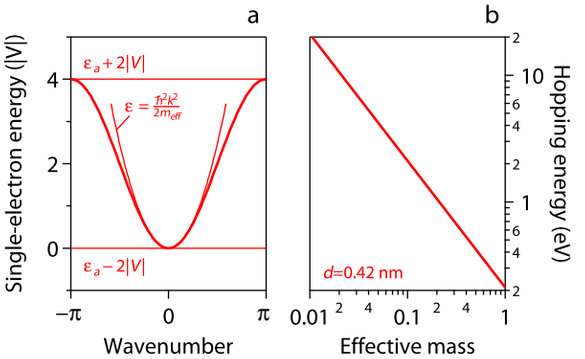

FIG. 17. Single-electron dispersion relation. (a) Energy band dispersion for the 1D, single-state atom chain, together with the best fitting parabola corresponding to the effective mass approximation. (b) Relation between the hopping energy and the effective mass of the electron, calculated for a lattice parameter $a = 0.42\,\mathrm{nm}$.

DATA AVAILABILITY STATEMENT

This study does not contain experimental data. Simulation protocols and results are available on request from the author.

Appendix A: Single Electrons on a 1D Chain

1. Constructing the Single-Electron Eigenstates

To establish single-electron states on an infinite 1D chain, we take as a basis states $|a_s\rangle$, which represent an electron localized on atom s, see Figure 16. In line with the Hückel model, we will assume that the states $(|a_0\rangle, |a_1\rangle, \ldots,)$ form an orthonormal basis. We accordingly expand the single-electron eigenstates – which we already label $|k\rangle$ – as:

$$|k\rangle = \sum_s c_{k,s}|a_s\rangle \tag{A1}$$

In principle, the expansion coefficients are found by solving the eigenvalue equation of the Hamiltonian. However, the resulting eigenstates must reflect the translational symmetry of the chain of atoms. More specifically, a leftward shift of the chain by one lattice parameter maps the chain on itself, while changing the expansion coefficient $c_{k,s}$ into $c_{k,s+1}$. However, as the Hamiltonian is invariant for such a translation, the leftward shift can change eigenstates by a phase factor $\exp(ik)$ at best. Hence:

$$c_{k,s+1} = e^{ik} c_{k,s} \tag{A2}$$

Identifying k with the wavenumber, we obtain the following set of Bloch waves as single-electron eigenstates on the chain:

$$|k\rangle = \frac{1}{\sqrt{N}} \sum_s e^{ik\cdot s}|a_s\rangle \tag{A3}$$

Note that we took here the lattice parameter as the unit of length and introduced the number of atoms N on the chain in this expression for the purpose of normalization. For completeness, we note that the expansion of the Bloch wave $|k\rangle$ in atom-localized states $|a_s\rangle$ can be inverted to yield:

$$|s\rangle = \frac{1}{\sqrt{N}} \sum_k e^{-ik\cdot s}|k\rangle \tag{A4}$$

2. Determining the Single-Electron Eigenenergies

Having the eigenstates $|k\rangle$, the corresponding eigenenergies ε_k are obtained as the expectation value of the Hamiltonian $\mathbf{H}$:

$$\varepsilon_k = \langle k|\mathbf{H}|k\rangle = \frac{1}{N}\sum_{s,s'} e^{-iks'}\langle s'|\mathbf{H}|s\rangle e^{iks} \tag{A5}$$

Note that the matrix elements $\langle s'|\mathbf{H}|s\rangle$ involve the basis states where the electron is located on atom s' and s, respectively. In line with the Hückel model, we will take all these matrix elements as zero, unless s' and s label the same or neighboring atoms. This leads to the so-called on-site and hopping matrix elements, which we write as:

$$\langle s|\mathbf{H}|s\rangle = \varepsilon_a \tag{A6}$$
$$\langle s-1|\mathbf{H}|s\rangle = \langle s+1|\mathbf{H}|s\rangle = V \tag{A7}$$

Using these two quantities, the eigenenergy ε_k reads:

$$\varepsilon_k = \varepsilon_a + V\left(e^{-ik} + e^{ik}\right) = \varepsilon_a + 2V\cos(k) \tag{A8}$$

We thus obtain the well-known dispersion of a single-state energy band, as illustrated in Figure 17a.

3. Relevance of the Single-Electron States

While somewhat academic as an example, we can use the 1D chain as a model to describe electron states in the conduction band of a semiconductor. This brings the bottom of the conduction band at $k = 0$, an often encountered situation in tetragonal semiconductors such as CdSe or InP. In the effective mass approximation, these bands are reduced the parabolas around the conduction-band minimum, with the curvature of the parabola related to the inverse of the effective mass of

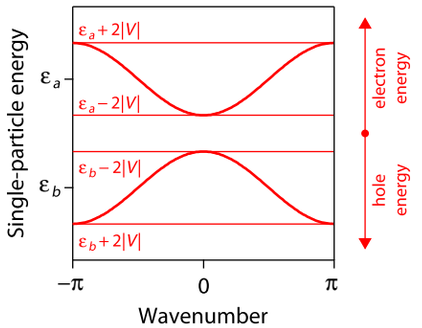

FIG. 18. Combined energy band dispersion for electron and hole states on the 1D, single-state atom chain. The plot was made assuming the same hopping matrix for electrons and holes.

the conduction-band electrons. Taking the unit of energy as $\hbar^2/m_e d^2$, with m_e the free electron mass, we have:

$$m^\star = \frac{1}{2|V|} \tag{A9}$$

As can be seen in Figure 17a, a chain with a higher $|V|$ will represent electrons with a smaller effective mass. Moreover, as shown in Figure 17b, setting $d = 0.42\,\text{nm}$, Eq A9 relates an effective mass $m^\star = 0.1$ to a hopping matrix element of 2 eV, a number we can use for referencing any energy expressed in units of $|V|$.

Note that the same 1D chain can be used to describe hole states in the valence band of a semiconductor. Since hole energies are the opposite of electron energies, we will obtain a band having an energy maximum at $k = 0$, and a hopping matrix element related to the hole effective mass. The resulting combined dispersion relation, with the hole energy indexed as b and the same hopping matrix for electrons and holes is represented in Figure 18.

Appendix B: Center-of-Mass and Internal Wavenumber

An electron-hole pair state constructed as the direct product of single-electon and single-hole Bloch waves will be characterized by expansion coefficients $c_{s,t}$ given by:

$$c_{s,t} = e^{i(k\cdot s + l\cdot t)} \tag{B1}$$

Expressing the same state using the center-of-mass R and the electron-hole distance r as coordinates will have the same expansion coefficients when the wavenumbers K and κ conjugate to R and r are taken such that:

$$K\cdot R + \kappa\cdot r = k\cdot s + l\cdot t \tag{B2}$$

Hence, we have:

$$\begin{aligned} K &= k + l \\ \kappa &= \tfrac{1}{2}(k-l) \end{aligned} \quad \Leftrightarrow \quad \begin{aligned} k &= \tfrac{K}{2} + \kappa \\ l &= \tfrac{K}{2} - \kappa \end{aligned} \tag{B3}$$

Appendix C: Chains with Different Electron and Hole Hopping Matrix Elements

The tight-binding model has been developed by taking the hopping matrix element for electrons and holes equal, a situation that yields electron-hole pairs with equal effective masses. This assumption simplifies the analytical formulas, but the approach is not limited to this specific case. In the more general case, which would describe electrons and holes with different effective masses, the two-particle Hamiltonian must be constructed using two hopping matrix elements:

$$\langle a_{s-1}\,|\,\mathbf{H}_e\,|\,a_s\rangle = V_e \tag{C1}$$
$$\langle b_{t-1}\,|\,\mathbf{H}_h\,|\,b_t\rangle = V_h \tag{C2}$$

These hopping matrix elements are related to the effective masses according to:

$$m_e^\star = \frac{1}{|V_e|} \tag{C3}$$
$$m_h^\star = \frac{1}{|V_h|} \tag{C4}$$

To illustrate the impact of these changes, we again derive the Hamiltonian matrix for the internal exciton motion on the infinite chain.

Since different hopping matrix elements do not change the overall symmetry requirement on the eigenstates, the states as described by Eq 10 can still be used as a basis for the internal Hamiltonian:

$$|K,r\rangle = \frac{1}{\sqrt{N}}\sum_R e^{iKR}|a_{R+\frac{r}{2}}, b_{R-\frac{r}{2}}\rangle \tag{C5}$$

Again, hopping of electrons and holes to neighboring atoms will couple states $|K,p\rangle$ and $|K,p+1\rangle$, and states $|K,p\rangle$ and $|K,p-1\rangle$. More specifically, the matrix element $\mathbf{H}_{K;p+1,p}$ will consist of a contribution $\langle K,p+1\,|\,\mathbf{H}\,|\,K,p\rangle_e$ due to an electron hopping to the right, and a contribution $\langle K,p+1\,|\,\mathbf{H}\,|\,K,p\rangle_h$ due to a hole hopping to the left. For the electron, hopping right changes the center-of-mass and relative coordinate by $1/2$ and 1, respectively. Hence, we have:

$$\begin{aligned} &\langle K,p+1\,|\,\mathbf{H}\,|\,K,p\rangle_e \\ &= \frac{1}{N}\sum_R e^{-i\frac{K}{2}}\langle a_{R+\frac{p+1}{2}}, b_{R-\frac{p}{2}}\,|\,\mathbf{H}\,|\,a_{R+\frac{p}{2}}, b_{R-\frac{p}{2}}\rangle = V_e e^{-i\frac{K}{2}} \end{aligned}$$

Similarly, for the hole, hopping left changes the center-of-mass and relative coordinate by $-1/2$ and 1, respectively. Hence, we have:

$$\begin{aligned} &\langle K,p+1\,|\,\mathbf{H}\,|\,K,p\rangle_h \\ &= \frac{1}{N}\sum_R e^{i\frac{K}{2}}\langle a_{R+\frac{p}{2}}, b_{R-\frac{p+1}{2}}\,|\,\mathbf{H}\,|\,a_{R+\frac{p}{2}}, b_{R-\frac{p+1}{2}}\rangle = V_h e^{i\frac{K}{2}} \end{aligned}$$

A similar reasoning can be applied to coupling due to the electron hopping left and the hole hopping right, which eventually yields the matrix elements of the internal Hamiltonian as:

$$\mathbf{H}_{K;p,p} = \varepsilon_{eh}(p) \tag{C6}$$
$$\mathbf{H}_{K;p+1,p} = V_e e^{-i\frac{K}{2}} + V_h e^{i\frac{K}{2}} \tag{C7}$$
$$\mathbf{H}_{K;p-1,p} = V_e e^{i\frac{K}{2}} + V_h e^{-i\frac{K}{2}} \tag{C8}$$

In the absence of electron-hole interaction, the eigenenergies are obtained as:

$$\begin{aligned}\varepsilon_{K,\kappa} &= \varepsilon_a + \varepsilon_b + 2V_e \cos\left(\frac{K}{2}+\kappa\right) + 2V_h \cos\left(\frac{K}{2}-\kappa\right) \\ &= \varepsilon_a + \varepsilon_b + 2V_e \cos(k) + 2V_h \cos(l)\end{aligned} \tag{C9}$$

This energy is the sum of the electron and hole energy in states characterized by the wavenumbers k and l.

For the Hamiltonian describing the electron and the hole interacting through a point-like interaction, the $K = 0$ states are obtained by replacing the off-diagonal matrix element $2V$ by $V_e + V_h$. Given the inverse relation between the coupling matrix elements and the effective mass of the electron and the hole, this change is tantamount to replacing the reduced mass $1/2m^\star$ by $1/m_e^\star + 1/m_h^\star$ in the expressions for ε_{X} and r_{X}.

Appendix D: Eigenstates for Electron Localization by Point Defects

If the on-site energy for the electron on one of the atoms is lower by an amount $\delta(\varepsilon)$ than all other on-site energies, a single electron Hamiltonian is obtained that strongly resembles the Hamiltonian describing the internal state of the electron-hole pair in the case of a point-like electron hole interaction. Labeling the position of the point defect as $s = 0$, the expansion coefficients $\psi_e(s)$ of the lowest energy state can be obtained using the following *Ansatz*:

$$\psi_e(s) = \phi_x(0) e^{-\frac{|s|}{s_{loc}}} \tag{D1}$$

Using these expansion coefficients, and setting $\varepsilon_a = 0$, the eigenvalue equation of the electron Hamiltonian is reduced to a set of two equations with the energy $\varepsilon_{e,loc}$ of the lowest energy eigenstate and the localization length s_{loc} as the two unknowns:

$$\left(-\delta(\varepsilon) - \varepsilon_{e,loc}\right) + 2Ve^{-\frac{1}{s_{loc}}} = 0 \tag{D2}$$

$$-\varepsilon_{e,loc} + V\left(e^{-\frac{1}{s_{loc}}} + e^{\frac{1}{s_{loc}}}\right) = 0 \tag{D3}$$

We thus obtain:

$$\varepsilon_{e,loc} = 2|V|\left(1 - \sqrt{1 + \frac{\delta(\varepsilon)^2}{4V^2}}\right) \tag{D4}$$

$$s_{loc} = \frac{1}{\operatorname{asinh}\left(\frac{\delta(\varepsilon)}{2|V|}\right)} \tag{D5}$$

Hence, we obtain a lowest-energy eigenstate that discribes an electron localized around the defect, and with an energy that is lower than the electron of the free electron state at the bottom of the conduction band. Clearly, localization and energy lowering are more pronounced the lower the on-site energy of the point defect, while a larger hopping matrix element – so a lower effective mass – counteracts the impact of localization.

Similarly, the coupling between two atoms is larger by an amount $\delta(V)$ than between any other pair of atoms, the expansion coefficients $\psi_e(s)$ of the lowest energy state can be obtained using the following *Ansatz*:

$$\psi_e(s) = \phi_x(0) e^{-\frac{|s-1/2|}{s_{loc}}} \tag{D6}$$

Here, we numbered the pair of atoms with the enhanced coupling as $s = 0$ and 1. Using these expansion coefficients, and setting $\varepsilon_a = 0$, the eigenvalue equation of the electron Hamiltonian is reduced to a set of two equations with the energy $\varepsilon_{e,loc}$ of the lowest energy eigenstate and the localization length s_{loc} as the two unknowns:

$$-\varepsilon_{e,loc} + (V + \delta(V)) + Ve^{-\frac{1}{s_{loc}}} = 0 \tag{D7}$$

$$-\varepsilon_{e,loc} + V\left(e^{-\frac{1}{s_{loc}}} + e^{\frac{1}{s_{loc}}}\right) = 0 \tag{D8}$$

We thus obtain:

$$\varepsilon_{e,loc} = -\frac{\delta(V)^2}{V + \delta(V)} \tag{D9}$$

$$s_{loc} = -\frac{1}{\ln\left(1 + \frac{\delta(V)}{V}\right)} \tag{D10}$$

Hence, we again find that larger deviations from the lattice periodicity will force a stronger localization, which will be counteracted by a larger hopping matrix element.

Appendix E: Sum Rule for Transition Dipole Moments

Within the basis of localized electron hole pair states $|a_s, b_t\rangle$, the transition dipole moment $D_{n;0}$ of an eigenstate $|n\rangle$ can be written as:

$$D_{n;0} = d_0 \sum_s c_{n,ss} = d_0\left(\mathbf{c}^{\mathrm{T}} \cdot \mathbf{d}\right) \tag{E1}$$

Here, $\mathbf{c}^{\mathrm{T}}$ is a row vector containing the expansion coefficients $c_{n,st}$, whereas $\mathbf{d}$ is a column vector containing a 1 for each position where $s = t$, and a 0 for all other positions. Hence, $D_{n;0}$ can also be written as:

$$D_{n;0} = d_0(\mathbf{C} \cdot \mathbf{d})_n \tag{E2}$$

Here, $\mathbf{C}$ is a matrix whose rows are filled with the expansion coefficients of the N^2 different exciton eigenstates; $D_{n;0}$ then corresponds to the entry at row n of the column vector $d_0\mathbf{C}\cdot\mathbf{d}$. We therefore have:

$$\sum_n D_{n;0}^2 = d_0^2\left(\mathbf{d}^{\mathrm{T}}\mathbf{C}^{\mathrm{T}}\mathbf{C}\mathbf{d}\right) \tag{E3}$$

Since $\mathbf{C}$ is a unitary matrix by construction, we have:

$$\sum_n D_{n;0}^2 = d_0^2\left(\mathbf{d}^{\mathrm{T}}\mathbf{d}\right) = d_0^2 N \tag{E4}$$

REFERENCES

[1]L. Brus, "A simple model for the ionization potential, electron affinity, and aqueous redox potentials of small semiconductor crystallites," J. Chem. Phys. **79**, 5566–5571 (1983).
[2]L. Brus, "Electron-electron and electron-hole interactions in small semiconductor crystallites - the size dependence of the lowest excited electronic state," J. Chem. Phys. **80**, 4403–4409 (1984).
[3]A. L. Efros and L. E. Brus, "Nanocrystal quantum dots: from discovery to modern development," ACS Nano **15**, 6192–6210 (2021).
[4]R. Burke, K. L. Bren, and T. D. Krauss, "Semiconductor nanocrystal photocatalysis for the production of solar fuels," J. Chem. Phys. **154**, 030901 (2021).
[5]M. V. Kovalenko, L. Manna, A. Cabot, Z. Hens, D. V. Talapin, C. R. Kagan, V. I. Klimov, A. L. Rogach, P. Reiss, D. J. Milliron, P. Guyot-Sionnnest, G. Konstantatos, W. J. Parak, T. Hyeon, B. A. Korgel, C. B. Murray, and W. Heiss, "Prospects of nanoscience with nanocrystals," ACS Nano **9**, 1012–1057 (2015).
[6]M. A. Becker, R. Vaxenburg, G. Nedelcu, P. C. Sercel, A. Shabaev, M. J. Mehl, J. G. Michopoulos, S. G. Lambrakos, N. Bernstein, J. L. Lyons, T. Stoferle, R. F. Mahrt, M. V. Kovalenko, D. J. Norris, G. Raino, and A. L. Efros, "Bright triplet excitons in caesium lead halide perovskites," Nature **553**, 189+ (2018).
[7]A. E. K. Kaplan, C. J. Krajewska, A. H. Proppe, W. Sun, T. Sverko, D. B. Berkinsky, H. Utzat, and M. G. Bawendi, "Hong-ou-mandel interference in colloidal $CsPbBr_3$ perovskite nanocrystals," Nat. Photonics **17**, 775–780 (2023).
[8]I. Tanghe, M. Samoli, I. Wagner, S. A. Cayan, A. H. Khan, K. Chen, J. Hodgkiss, I. Moreels, D. V. Thourhout, Z. Hens, and P. Geiregat, "Optical gain and lasing from bulk cadmium sulfide nanocrystals through bandgap renormalization," Nat. Nanotech. **18**, 1423–1429 (2023).
[9]M. Nasilowski, B. Mahler, E. Lhuillier, S. Ithurria, and B. Dubertret, "Two-dimensional colloidal nanocrystals," Chem. Rev. **116**, 10934–10982 (2016).
[10]P. Geiregat, C. Roda, I. Tanghe, S. Singh, A. Di Giacomo, D. Lebrun, G. Grimaldi, J. Maes, D. Van Thourhout, I. Moreels, A. J. Houtepen, and Z. Hens, "Localization-limited exciton oscillator strength in colloidal CdSe nanoplatelets revealed by the optically induced stark effect," Light-Sci. Appl. **10**, 112 (2021).
[11]S. Stobbe, T. W. Schlereth, S. Höfling, A. Forchel, J. M. Hvam, and P. Lodahl, "Large quantum dots with small oscillator strength," Phys. Rev. B **82**, 233302 (2010).
[12]Z. Hens and I. Moreels, "Light absorption by colloidal semiconductor quantum dots," J. Mat. Chem. **22**, 10406–10415 (2012).
[13]K. Ishida, H. Aoki, and T. Chikyu, "One-dimensional exciton in a two-band tight-binding model with long-range interactions," Phys. Rev. B **47**, 7594–7597 (1993).
[14]G. W. Bryant, "Hubbard model for intermediate-dimensional excitons," Phys. Rev. B **49**, 16129–16140 (1994).
[15]U. Peschel, M. Thümmler, T. Lettau, S. Gräfe, and K. Busch, "Two-particle tight-binding description of higher-harmonic generation in semiconductor nanostructures," Phys. Rev. B **106**, 245307 (2022).
[16]W. A. Harrison, *Solid State Theory* (Dover Publications, Inc., 1980).
[17]F. H. L. Essler, H. Frahm, F. Göhmann, A. Klümper, and V. E. Korepin, *The One-Dimensional Hubbard Model* (Cambridge University Press, 2005).
[18]W. Harrison, "Tight-binding theory of surface states in metals," Phys. Scripta **67**, 253–259 (2003).
[19]A. Efros, M. Rosen, M. Kuno, M. Nirmal, D. Norris, and M. Bawendi, "Band-edge exciton in quantum dots of semiconductors with a degenerate valence band: Dark and bright exciton states," Phys. Rev. B **54**, 4843–4856 (1996).
[20]T. Aubert, A. A. Golovatenko, M. Samoli, L. Lermusiaux, T. Zinn, B. Abecassis, A. Rodina, V, and Z. Hens, "General expression for the size-dependent optical properties of quantum dots," Nano Lett. **22**, 1778–1785 (2022).
[21]R. Elliott, "Intensity of optical absorption by excitons," Phys. Rev. **108**, 1384–1389 (1957).
[22]J. Feldmann, G. Peter, E. Gobel, P. Dawson, K. Moore, C. Foxon, and R. Elliott, "Linewidth dependence of radiative exciton lifetimes in quantum-wells," Phys. Rev. Lett. **59**, 2337–2340 (1987).